A FRET-Based Calcium Biosensor with Fast Signal Kinetics and High Fluorescence Change

Marco Mank,* Dierk F. Reiff,† Nicola Heim,* Michael W. Friedrich,* Alexander Borst,† and Oliver Griesbeck*
*AG Zelluläre Dynamik, †Abteilung Neuronale Informationsverarbeitung, Max-Planck-Institut für Neurobiologie 82152 Martinsried, Germany

ABSTRACT Genetically encoded calcium biosensors have become valuable tools in cell biology and neuroscience, but some aspects such as signal strength and response kinetics still need improvement. Here we report the generation of a FRET-based calcium biosensor employing troponin C as calcium-binding moiety that is fast, is stable in imaging experiments, and shows a significantly enhanced fluorescence change. These improvements were achieved by engineering magnesium and calcium-binding properties within the C-terminal lobe of troponin C and by the incorporation of circularly permuted variants of the green fluorescent protein. This sensor named TN-XL shows a maximum fractional fluorescence change of 400% in its emission ratio and linear response properties over an expanded calcium regime. When imaged in vivo at presynaptic motoneuron terminals of transgenic fruit flies, TN-XL exhibits highly reproducible fluorescence signals with the fastest rise and decay times of all calcium biosensors known so far.

INTRODUCTION

Biosensors based on the green fluorescent protein (GFP) have become valuable tools in cell biology and neuroscience (1–3). Genetically encoded calcium indicators (GECIs) especially have been used successfully in a variety of cell types and in the nervous system of transgenic organisms ranging from nematodes (4,5) to fruit flies (6–9), zebrafish (10), and recently also mice (11,12). However, these studies revealed that the field could benefit from a number of improvements including faster kinetics and bigger calcium-induced fluorescence changes. In particular double chromophore indicators employing fluorescence resonance energy transfer (FRET) between cyan fluorescent protein (CFP) and variants of yellow fluorescent protein (YFP) showed slow off-rate kinetics (9,13), which is a drawback in using these sensors in the nervous system as much temporal information on calcium signaling is lost. Single fluorophore sensors are somewhat faster but suffer from reduced photostability, complex photophysics, pH sensitivity, and in some cases reduced folding efficiency at 37°C (9,12,14–16).

We recently created a new generation of calcium biosensors that instead of using the highly regulated calmodulin employ variants of troponin C (TnC)—the specialized calcium sensor of skeletal and cardiac muscle—as calcium-binding moieties. These sensors are believed to be minimally perturbing as they do not interfere with the host cell biochemistry and work in subcellular targetings in which previous calmodulin-based sensors tended to fail (13). TnC consists of a regulatory, calcium-specific N-terminal lobe and a C-terminal lobe with two additional calcium-binding sites that are considered to have predominantly structural functions and competitively bind magnesium (17). These C-terminal EF-hands have ~100-fold slower calcium off-rates compared to the N-terminal hands and complex kinetics as they are partially bound by magnesium ions at resting state which are exchanged by calcium ions after stimulation (18,19). Here we demonstrate that we can improve the specificity and response kinetics of TnC-based sensors by engineering the magnesium- and calcium-binding properties within the C-terminal lobe. In addition, we took advantage of recent work with circularly permuted fluorescent proteins (20–22) to increase the maximal fluorescence change. One of these sensors, TN-XL (for X-large) has a maximal fluorescence change of over 400% change in its emission ratio from zero calcium to calcium saturation in vitro, a fast off-rate, and a stable and reproducible performance. At the neuromuscular junction (NMJ) of transgenic fruit flies, TN-XL shows the fastest response kinetics of all GECIs known so far. Thus, the combination of increased ion selectivity, moderate calcium sensitivity, and strongly increased maximum fluorescence change makes this calcium biosensor a useful tool for in vivo imaging experiments with improved signal size, stability, and temporal resolution.

MATERIAL AND METHODS

Gene construction

Circularly permuted (cp) variants of the fluorescent proteins were obtained by cloning two fragments that were created by polymerase chain reaction into pRSETB (Invitrogen, Carlsbad, CA). The first fragment starts with the indicated amino acid residue where an additional Met was placed in front. The second fragment contains a GGSGGT linker before starting with the original Met of the protein and ends at the indicated position-1. An additional stop codon was placed at the end of each permuted variant. The indicated position is resembled by the figure of the cp variant. For replacing the donor/acceptor fluorophores in TN-L15 cerulean, cerulean cp174, cerulean cp158, citrine cp174, and citrine cp158 were used. Donors were cloned into TN-L15 by using *Bam*HI/*Sph*I restriction sites, whereas acceptors were cloned by

Submitted August 30, 2005, and accepted for publication November 7, 2005.

Address reprint requests to Oliver Griesbeck, E-mail: griesbeck@neuro.mpg.de.

0006-3495/06/03/1790/07 $2.00

doi: 10.1529/biophysj.105.073536

using *Sac*I/*Eco*RI restriction sites. Mutations were introduced by site-directed mutagenesis using the primer extension method (Stratagene, La Jolla, CA). For protein expression in mammalian cells, an optimized Kozak consensus sequence (GCC GCC ACC ATG G) was introduced at the 5′ end of CFP. The indicator was subcloned between the *Bam*HI/*Eco*RI restriction sites of pcDNA3 (Invitrogen).

Protein expression, in vitro spectroscopy, and titrations

Proteins were expressed in *Escherichia coli* BL21 and purified as described previously (13). Protein concentrations were determined in 6 M guanidinium hydrochloride at 280 nm in a Varian (Palo Alto, CA) absorption photometer. Corresponding extinction coefficients were obtained by using the Protparam Tool (http://www.expasy.org/tools/protparam.html). Calcium titrations were done with premixed calcium buffers (calcium calibration kit No. 1 with 1 mM magnesium, Molecular Probes, Eugene, OR). Curves were normalized to the value at 39.8 μM free Ca^{2+}. Dissociation kinetics were measured with a stopped-flow RX2000 rapid kinetics accessory unit (Applied Photophysics, Leatherhead, UK) at a Cary Eclipse fluorometer (Varian). A total of 200 nM of protein in 10 mM 3-morpholinopropane sulfonic acid (MOPS)/50 mM KCl/4 mM $CaCl_2$/2 mM $MgCl_2$ pH 7.5 was mixed with 10 mM MOPS/50 mM KCl/20 mM 1,2-bis-(o-aminophenoxy) ethane-*N*,*N*,*N*′,*N*′, tetraacedic acid (BAPTA) (tetrapotassium salt) pH 7.5. The reaction mixture was excited at 432 nm and emission was taken at 475 nm or 527 nm, respectively. At least nine measurements per protein per channel were taken to calculate the decay of the 527/475 nm ratio. The resulting time constant of the indicator was built by the average of three independent measurements.

Cell culture and imaging

Hippocampal neurons were prepared from 18-day-old rat embryos (E18). Neurons were plated on glass-bottomed dishes (MatTek, Ashland, MA) and transfected by calcium-phosphate precipitation. Imaging of the neurons was started at least 2 days after transfection in Hanks' buffered saline solution pH 7.2. Stimulation of the neurons was achieved by raising extracellular potassium to 50 mM while preserving osmolality. The imaging setup consists of a Zeiss (Jena, Germany) Axiovert 35M microscope, a 440/20 excitation filter, a 455 dichroic long-pass mirror, and two emission filters (485/35 for CFP and 535/25 for citrine). The setup was controlled by Metafluor version 4.6 software (Universal Imaging, West Chester, PA). Pictures were taken by a charge-coupled device camera (CoolSnap, Roper Scientific, Trenton, NJ).

Transgenic flies and imaging

The cDNA of TN-XL was subcloned into the Not I site of the pUAST vector (23) and inserted into the *Drosophila* genome of white$^-$ flies (w$^-$, ''Bayreuth'', kindly provided by Christian Lehner, Bayreuth, Germany) by P-element mediated germ line transfection (24). The Gal4/UAS system (23) was used to direct the expression of TN-XL to neurons and the larval NMJ. Experimental animals were generated by crossing male *UAS-TN-XL* flies to female *elav*C^{155}-*Gal*4 flies (25). All animals were raised on standard corn medium supplemented with fresh yeast at 25°C. Female, late third instar larvae were selected for the imaging of calcium-induced presynaptic fluorescence changes. The larval preparation, solutions, setup, and imaging of NMJs at muscle 6/7 was done as described in Reiff et al. (9). In short, TN-XL was excited at 430 nm, and a neutral density filter (0.4) was used to reduce the excitation energy. A dichroic mirror (DC455LP, Chroma, Brattleboro, VT) was used to separate excitation from emission light. The emitted light was further split (DC515, Chroma) and simultaneously imaged by using a beam splitter and subsequent charge-coupled device camera (9). In most experiments calcium was adjusted to 1.5 mM and electric stimuli were applied at different frequencies for 2.2 s. For saturation of the FRET signal the calcium concentration was increased to 10 mM. The fractional ratio change was calculated after subtraction of the intensity of a nearby background region from the intensity of an individual bouton in each emission channel individually. Subsequently the ratio (R) of both emission intensities and its fractional change ($\Delta R/R$) was calculated (9). (In Fig. 4 *C*, Table 2, and the Supplementary Fig. 2, the TN-XL fluorescence signals were compared to data from previous experiments (9). Please note that data from Reiff et al. (9) were recorded without neutral density filters. Therefore in direct comparisons, TN-XL traces can appear slightly noisier.)

RESULTS

We generated a number of permuted variants of CFP, cerulean (26), or the acceptor protein citrine (27), taking advantage of previous reports on circular permutations of various GFPs (20–22) (Supplementary Fig. 1, *A* and *B*). Permuted versions of citrine differed considerably in expression properties and brightness (Supplementary Fig. 1, *C* and *D*). Cp117, cp103, cp50, cp39, and cp25 did not show comparable brightness to nonpermuted citrine when expressed in *E. coli* (Supplementary Fig. 1, *C* and *D*) and were therefore not considered further in this study. However, citrine cp174 and citrine cp158 yielded excitation and emission maxima, pKas, and quantum yields similar to the original citrine (Supplementary Table 1). Ultimately we were interested in whether such permuted fluorescent proteins had any influence on the response characteristics of genetically encoded TnC-based biosensors that employ intramolecular FRET between GFPs. We inserted combinations of permuted citrine and CFP/cerulean into TN-L15, a genetically encoded calcium sensor based on chicken skeletal muscle TnC (csTnC) (13). A summary of effects of various donor and acceptor combinations on signal strength of the resulting indicator is given in Table 1, with the number, in percent,

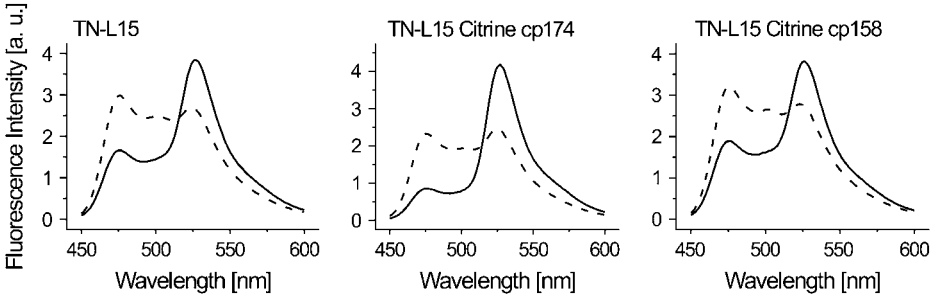

FIGURE 1 In vitro emission spectra of TN-L15, TN-L15 citrine cp174, and TN-L15 citrine cp158. Emission spectra of the various indicators are shown at 25 μM EGTA (*dashed line*) and 10 mM $CaCl_2$ (*solid line*) in 100 mM KCL/10 mM MOPS pH 7.5. Emission was taken from 450 to 600 nm with an excitation at 432 nm.

TABLE 1 Effects of donor and acceptor replacements on maximum ligand-induced change in emission ratio in TN-L15

Acceptor/donor	Citrine	Citrine cp174	Citrine cp158
ECFP	140%	400%	140%
Cerulean	90%	130%	100%
Cerulean cp174	70%	120%	90%
Cerulean cp158	80%	80%	80%

The table shows the $\Delta R/R$s of the indicated constructs. Values were calculated by the difference of 527/475 nm ratio after saturation with 10 mM $CaCl_2$ without Mg^{2+} in 100 mM KCL/10 mM MOPS/25 μM EGTA, pH 7.5.

indicating the maximal change in 527/475 nm emission ratio from zero calcium to calcium saturation. Replacing citrine by citrine cp174 within TN-L15 dramatically increased the maximal fluorescence change of the indicator from 140% to maximally 400% ratio change from zero calcium to calcium saturation in the absence of magnesium. Most of this was due to an increased absorbance of excited state energy by citrine cp174, which resulted in a drastic reduction of CFP emission under conditions of calcium saturation (Fig. 1). Varying the permutation of citrine by one amino acid to citrine cp173 and citrine cp175 did not result in further increases in performance compared to TN-L15 citrine cp174 (data not shown). Other combinations of permuted donor and acceptor proteins either were similar to TN-L15 in performance or worse (Table 1). No significant improvements were detectable by substitution of the donor, probably because CFP/cerulean had already been engineered for this purpose by deleting the 11 C-terminal amino acids to optimize FRET (Table 1). Substitutions of CFP with cerulean, a brighter variant of CFP with higher extinction coefficient and quantum yield, resulted in smaller fluorescence changes (Table 1) because the relative decrease in cerulean emission turned out to be smaller than the decrease in CFP emission. When employing a similar strategy to tune TN-humTnC, a related sensor based on human cardiac TnC (13), improvements were only moderate, increasing the fluorescence change of the sensor from 120% to 130% maximal change in emission ratio in TN-humTnC citrine cp174 (data not shown).

TN-L15 citrine cp174 was functional in HEK 293 cells, although the maximal fluorescence change from zero calcium to calcium saturation was reduced to 160%, presumably due to magnesium binding to the sensor at resting state. Magnesium binding at physiological concentrations resulted in increased FRET already at conditions of zero calcium within the purified protein, thus reducing the overall signal obtainable with calcium (Fig. 2 *C*). To preserve the full signal strength of the sensors in living cells, we therefore set out to eliminate competitive magnesium binding while

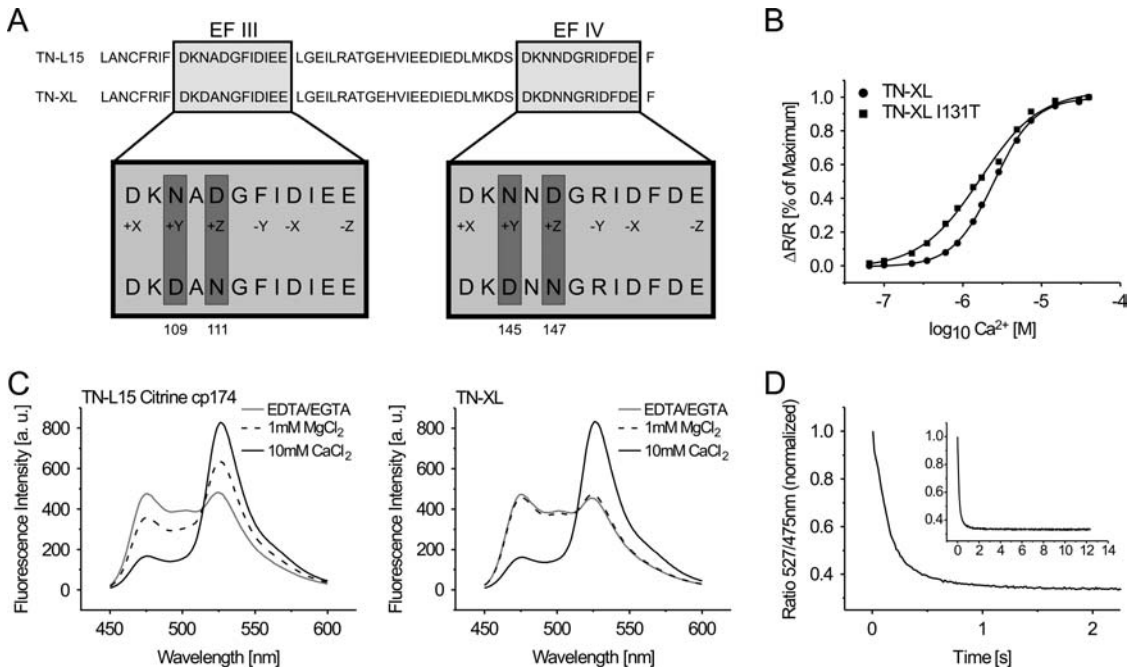

FIGURE 2 In vitro characteristics of TN-XL and TN-L15 citrine cp174. (*A*) Scheme of the substitutions of amino acids in the C-terminal part of the calcium-binding moiety of TN-XL. Shown are the calcium-binding loops of EF-hands III and IV. (*B*) Calcium titration curves of TN-XL and TN-XL I131T. Apparent K_ds are 2.5 μM for TN-XL and 1.7 μM for TN-XL I131T. (*C*) Emission spectra of TN-L15 citrine cp174 and TN-XL at 100 μM EDTA/25 μM EGTA (*gray line*), 1 mM $MgCl_2$ (*black dashed line*), and 10 mM $CaCl_2$/1 mM $MgCl_2$ (*black solid line*). Note that the magnesium-induced change in FRET detectable in TN-L15 citrine cp174 is absent in TN-XL. (*D*) Dissociation kinetics of TN-XL. A stopped-flow chamber setup coupled to a fluorometer was used to mix calcium-saturated indicator with 10 mM MOPS/50 mM KCl/20 mM BAPTA (tetrapotassium salt) pH 7.5. The decay of citrine emission or the increase in CFP emission was followed over time and the ratio calculated. The inset shows the same ratio trace within a longer time period of up to 12 s. The in vitro decay time constant was obtained from three independent normalized measurements of 527/475 nm ratio.

preserving calcium binding. Metal binding to TnC has been studied extensively (18,28–30). EF-hands III and IV were considered crucial targets to optimize ion selectivity and kinetics. The canonical EF-hand motif consists of two helices flanking a 12-residue cation-binding loop. Chelating residues in positions 1 (+x), 3 (+y), 5 (+z), 7 (−y), 9 (−x), and 12 (−z) (Fig. 2 *A*) ligate calcium through seven oxygen atoms in the three-dimensional array of a trigonal bipyramid. The smaller magnesium ion is chelated by some of the same residues, although only six oxygens are involved. A number of mutagenesis studies in TnC and calmodulin (31,32) as well as analysis of metal-binding properties of synthetic EF-hands (33) suggested that pairs of acidic amino acid residues at positions +z and –z are essential in conferring magnesium binding to EF-hands. We therefore eliminated the z-acid pairs found in TnC EF-hands III and IV by replacing the aspartate at position +z (Fig. 2 *A*). Simple mutagenesis of D^{111} and D^{147} significantly reduced magnesium interference while it slightly lowered calcium affinity. To counter the effect of lowering the Kd for calcium, we introduced additional acids replacing asparagines 109 and 145 with aspartates, the residues found in this position in EF-hands III and IV of calmodulin (34). Thus we ended up with double mutations within each hand III and IV, with mutations N^{145D}/D^{147N} having a smaller effect on magnesium-induced conformational change than mutations N^{109D}/D^{111N}. This suggests that EF-hand III was responsible for most of the magnesium-induced conformational change in TN-L15 citrine cp174. Alternatively, we also replaced the 12 amino acid chelating loop of EF-hand IV of TnC (csTnC) with the corresponding loop of EF-hand IV of calmodulin. This protein was similarly functional but provided no additional advantage and was therefore not considered further (data not shown). Combining mutations N^{109D}/D^{111N} and N^{145D}/D^{147N} resulted in a sensor in which the magnesium-induced change in FRET efficiency was abolished (Fig. 2 *C*). This sensor was named TN-XL. We characterized the calcium binding of TN-XL in more detail. Its Kd was determined to be 2.5 μM (Fig. 2 *B*) with a Hill slope of 1.7. Using a stopped-flow setup we investigated the off-kinetics of the sensor. Its off-rate was extremely fast, optimally fitted with a double exponential with a dominating τ of 142 ms (A_1 = 0.63) and a minor τ of 867 ms (A_2 = 0.06) (Fig. 2 *D*). Mutation of the N-cap residue 131 of helix G within TnC from isoleucine to threonine (35) yielded an indicator of higher calcium affinity with a Kd of 1.7 μM (Fig. 2 *B*) and shifted the Hill slope to 1.1, although at reduced maximal fluorescence change of 270%. TN-XL expressed well in primary hippocampal neurons at 37°C. Fluorescence was evenly distributed, filling all neuronal processes, with no signs of aggregation (Fig. 3 *C*). The nucleus was devoid of fluorescence. Repeated stimulations with high potassium followed by repeated washouts demonstrated stable baselines over long recording sessions and reproducible signals after stimulation. Moreover the signals induced by high potassium were more than doubled compared to TN-L15 (Fig. 3).

The most critical test in determining the function of a biosensor is its in vivo performance in cells and subcellular compartments of interest. To examine the exhibited fluorescence changes of TN-XL in neurons of living animals, transgenic *Drosophila* flies were engineered that enable the expression of TN-XL under control of an upstream activation sequence (UAS) (23). Using the panneural promoter C^{155} to drive Gal4 expression allowed for the optical imaging of presynaptic boutons at individual NMJs of *Drosophila* larvae (see Materials and Methods). In this preparation, axons and boutons expressing TN-XL were readily identifiable (Fig. 4 *A*). Electric stimulation of the nerve harboring the innervating axon evoked reliable fluorescence changes (Fig. 4 *B*) with an unusual fast time course compared to other double chromophore and even single chromophore

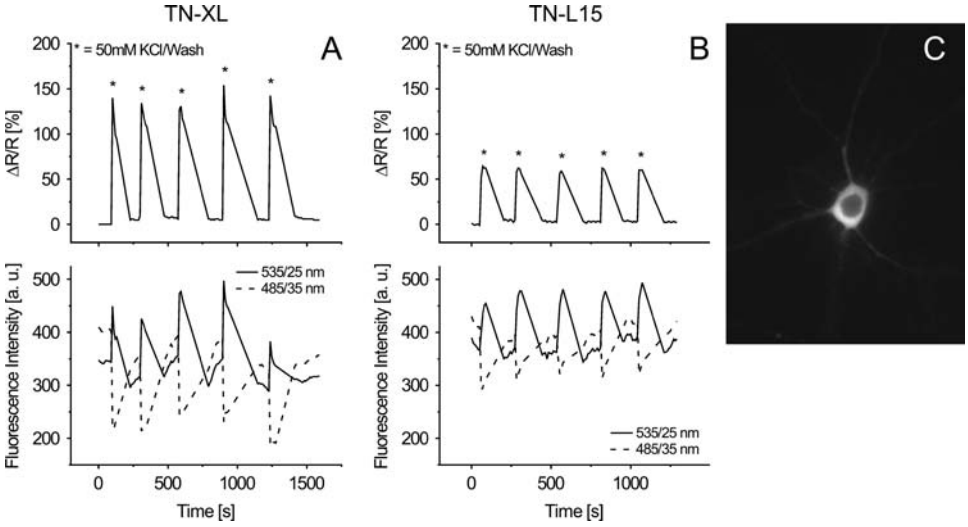

FIGURE 3 Performance of TN-XL and TN-L15 in primary hippocampal neurons. (*A*) Traces obtained from a rat hippocampal neuron transfected with TN-XL. Upper trace shows the changes of the normalized ratio. The cell was repeatedly stimulated by high potassium (50 mM) followed by washout. Lower trace shows the corresponding changes in the intensities of the YFP (535/25 nm) and the CFP (485/35 nm) channel. Time axis for ratio and intensities has the same scale. (*B*) Responses of a primary hippocampal neuron transfected with TN-L15 treated like *A*. (*C*) Primary hippocampal neuron expressing TN-XL. The image shows the citrine cp174 emission at 535/25 nm upon excitation at 440/20 nm. Scale bar, 10 μm.

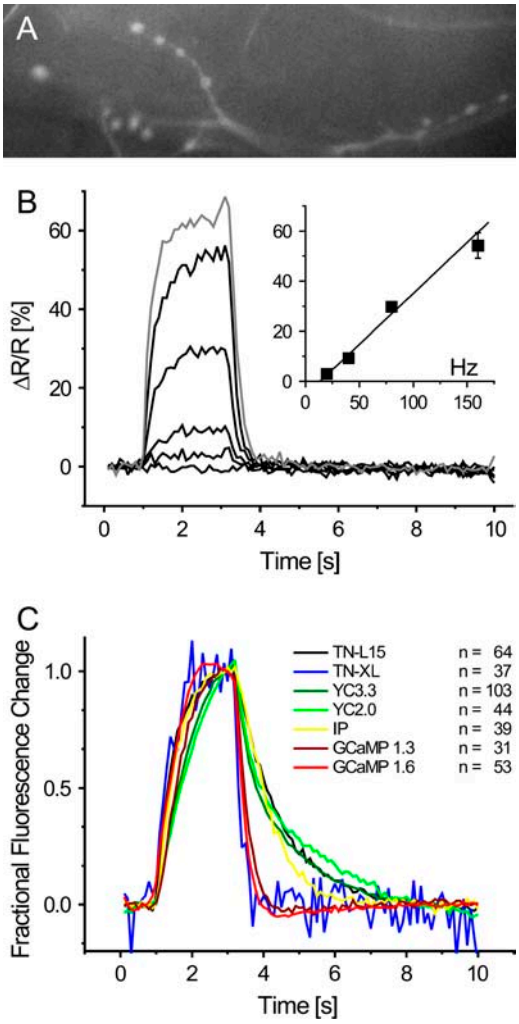

FIGURE 4 Rapid and linear changes of the TN-XL fluorescence in *Drosophila* in vivo. (*A*) TN-XL expression highlights presynaptic boutons at a transgenic *Drosophila* NMJ (raw intensity of citrine cp174 emission). Scale bar, 10 μm. (*B*) The TN-XL fluorescence exhibited staircase-like changes ($\Delta R/R$) at all stimulation frequencies (20, 40, 80, and 160 Hz for 2.2 s, *black traces*). Increasing the external calcium concentration from 1.5 to 10 mM only moderately increased $\Delta R/R$ at 160 Hz stimulation (*gray trace*). The control experiments without stimulation as well as the time periods before and after stimulation show a remarkably stable TN-XL signal. Action potential (AP) rates of 20 and up to 160 Hz were reported by a fairly linear increase in $\Delta R/R$ (*inset*). (*C*) Comparison of TN-XL (*blue trace*) to six other GECI response kinetics using identical stimulus conditions (AP-frequency 40 Hz, 2.2 s). In TN-XL, the strong improvement in the kinetics of the rise achieved in TN-L15 is retained and combined to a dramatic shortening of the time necessary for the fluorescence signals to decay. The corresponding time constants are given in Table 2. Single fluorophore sensor traces show fractional fluorescence changes and ratiometric indicator traces fractional ratio changes, all normalized to the maximum value.

indicators (Fig. 4 *C*, Table 2, and Supplementary Fig. 2). Action potential trains at increasing frequency evoked changes in the fractional change of the fluorescence ratio ($\Delta R/R$) with a fairly linear relationship to the actual stimulus frequency (Fig. 4 *B*, *inset*). Stimulation at 20, 40, 80, and 160 Hz evoked a $\Delta R/R$ of 2.9% ± 0.5%, 9.3% ± 0.8%, 29.7% ± 1.9%, and 54.2% ± 5.1% at 1.5 mM calcium in the external solution (Fig. 4 *B*, *black traces*, three NMJs, $n = 37$ boutons). At 160 Hz stimulation saturation of the probe is almost absent. However, increasing the calcium concentration to 10 mM (Fig. 4 *B*, *gray trace*) only moderately increased the observed signal change at 160 Hz ($\Delta R/R$ = 64.8% ± 3.7%, three NMJs, 37 boutons). Thus, 65% $\Delta R/R$ seems to represent the maximum observable fluorescence change in vivo under our experimental conditions. $\Delta R/R$ of individual boutons exhibited almost a staircase time course with time constants of 430 ms for the rise (40 Hz stimulation, single exponential fit) and 240 ms for the decay of the fluorescence signals. To demonstrate the improvements in response kinetics compared to previous FRET-based calcium biosensors and other single fluorophore sensors, imaging traces using TN-XL and a collection of previously published sensors, consisting of TN-L15 (13), Yellow Cameleon 2.0 and 3.3 (27,36), Inverse Pericam (IP) (37), and G-CaMP 1.3 (14) and 1.6 (38) obtained with identical stimulation patterns (40 Hz stimulation, 2.2 s) were plotted in the same graph (Fig. 4 *C*). The TN-XL, TN-L15, and YC2.0 data are not corrected for bleaching. All other indicators were corrected for bleaching as described in Reiff et al. (9). Table 2 summarizes rise and decay times of all of these sensors assayed under comparable conditions at the *Drosophila* NMJ in vivo. As can be seen in Table 2, TN-XL dramatically outmatches previous calmodulin-based FRET sensors such as YC2.0 and YC3.3 both in rise and decay times. Also single fluorophore sensors such as IP and G-CaMP 1.3 and 1.6 were slower than TN-XL both in rise and decay constants. Supplementary Fig. 2 shows the rise and decay phases of the indicator traces of Fig. 4 *C* at an extended temporal scale. Besides the above described fluorescence characteristics, the exhibited fluorescence changes of TN-XL were accompanied by remarkably stable fluorescence before and from shortly after the stimulus

TABLE 2 Time constant τ for the rise and the decay of indicator fluorescence signals at the *Drosophila* NMJ in vivo

Indicator	Rise (ms)	Decay (ms)
TN-L15	500	1330
TN-XL	430	240
YC3.3	1130	490/1780
YC2.0	1560	350/3070
IP	590	940
GCaMP1.3	810	330
GCaMP1.6	560	260

TN-XL exhibited by far the shortest time constants of all ratiometric indicators as well as of the single chromophore indicators IP and GCaMP1.3. Only the kinetics of the rise and decay of the GCaMP1.6 fluorescence changes were comparable or only moderately slower, respectively. All fits were done on the data shown in Fig. 4 *C* by using single exponential functions. The decay of YC2.0 and YC3.3 had to be fit by a double exponential function. Presynaptic action potentials were evoked at a rate of 40 Hz, which does not cause saturation of the individual indicator under these conditions (9). Close-ups of the rise and fall are shown in the Supplementary Fig. 2.

period on. None of the data shown for TN-XL is corrected for bleaching of the chromophores.

DISCUSSION

Above we reported the generation of a FRET-based calcium biosensor employing TnC as calcium-binding moiety that is fast, is stable in imaging experiments, and shows a significantly enhanced fluorescence change. Its off-rate is significantly faster than those of previous double chromophore sensors (Figs. 2 *D* and 4 *C*) and even outmatches the fastest single fluorophore sensors to date (9). TN-XL has stable and reproducible fluorescence properties, is pH insensitive in the physiological range due to the combination CFP/citrine, folds well at room temperature and at 37°C, and offers the benefits of ratiometric imaging. The key in achieving speed and ion selectivity of this sensor resided in engineering the EF-hands III and IV within the C-terminal lobe of csTnC. These C-terminal EF-hands have ~100-fold slower calcium off-rates compared to the N-terminal hands and complex kinetics as they are partially bound by magnesium ions at the resting state which are displaced by calcium ions after stimulation (18,19). Magnesium binding to these sites also induced a conformational change and concomitantly an increase in FRET efficiency, which diminished the maximal signal change obtainable by calcium (Fig. 2 *C*). Magnesium binding to EF-hands and discrimination of calcium versus magnesium are only beginning to be understood. The typical EF-hand motif consists of two helices that flank a loop of 12 amino acid residues responsible for cation binding. Chelating residues in positions 1 (+x), 3 (+y), 5 (+z), 7 (−y), 9 (−x), and 12 (−z) (Fig. 2 *A*) ligate calcium through seven oxygen atoms. The smaller magnesium ion is chelated by some of the same residues, although only six oxygens are involved. In synthetic EF-hands magnesium binding could be observed when negatively charged acids glutamate or aspartate formed z-acid pairs, chelating residues in positions +z and –z (33). Introducing a z-acid pair turned the calcium-specific first EF-hand of csTnC into one that competitively binds magnesium (32). Removing a z-acid pair from the first EF-hand of calmodulin severely attenuated magnesium binding while only moderately reducing calcium affinity (31). In line with these findings, removing z-acid pairs in sites III and IV of csTnC almost completely abolished magnesium-induced change in FRET in this sensor (Fig. 2 *C*) Combined with a modest decrease of the calcium affinity of the sensor to a Kd for calcium of 2.5 μM (Fig. 2 *B*), the kinetics was significantly sped up. Sensors with higher affinities are however also desirable for some applications. Interestingly, a number of calcium-sensitizing effects of mutating hydrophobic residues outside of the chelating binding loops of TnC have been described. Along these lines the mutation I^{131T} (35) increased the Kd of the sensor to 1.7 μM (Fig. 2 *B*).

By trying multiple combinations of circularly permuted donor and acceptor proteins, we succeeded in enhancing the maximal fluorescence change to 400% change in emission ratio. Recently, a calmodulin-based biosensor was described that showed an expanded fluorescence change of up to 560% change in emission ratio by incorporating circularly permuted versions of the acceptor protein Venus, another YFP variant (22). Interestingly, the similar permutations Venus cp173 and citrine cp174 were responsible for enhancing the responses of sensors employing the different calcium-binding moieties calmodulin-M13 or TnC. Permutation 173/174/175 allows the most dramatic rearrangement of the β-barrel when fused to another protein compared to the orientation of the nonpermuted protein fused in the identical manner. Therefore a more favorable orientation is the likely cause for the different FRET results in biosensors as well as in simple donor-acceptor fusions, whereas the slightly increased extinction coefficient of citrine cp174 compared to citrine (Supplementary Table 1) probably plays a negligible role. It is still unclear whether this can be regarded as a general rule as TN-humTnC was only modestly improved by insertion of citrine cp174. Therefore, adopting this tuning strategy to other sensors will be informative. Replacing CFP with cerulean, a brighter variant with higher extinction coefficient and quantum yield, resulted in sensors with smaller maximal fluorescence changes (Table 1) because the fractional decrease in cerulean fluorescence was smaller than for CFP.

Calcium biosensors based on variants of TnC are believed to be minimally interfering with the host cell biochemistry as they rely on a specialized calcium-binding protein that is not involved in signal transduction as calmodulin. Calmodulin binds and activates numerous target proteins, is phosphorylated extensively, and is sequestered by a plethora of calmodulin-binding proteins (39). Therefore many possible applications may be hampered by interactions of calmodulin-based sensors with these regulatory components. TnC-based sensors are functional in subcellular targetings in which other sensors tended to fail (13) and when expressed in the brain of transgenic mice (N. Heim, and O. Griesbeck, unpublished observations). Thus, these indicators appear to be suitable tools for in vivo imaging experiments in vertebrates as well as invertebrates.

SUPPLEMENTARY MATERIAL

An online supplement to this article can be found by visiting BJ Online at http://www.biophysj.org.

We thank Anja Schulze-Schenke for technical assistance.

This work was supported by the Max-Planck-Society and DFG priority programme SP1172.

REFERENCES

1. Zhang, J., R. E. Campbell, A. Y. Ting, and R. Y. Tsien. 2002. Creating new fluorescent probes for cell biology. *Nat. Rev. Mol. Cell Biol.* 3: 906–918.

2. Miyawaki, A. 2003. Visualization of the spatial and temporal dynamics of intracellular signaling. *Dev. Cell.* 4:295–305.
3. Griesbeck, O. 2004. Fluorescent proteins as sensors for cellular functions. *Curr. Opin. Neurobiol.* 14:636–641.
4. Suzuki, H., R. Kerr, L. Bianchi, C. Frokjaer-Jensen, D. Slone, J. Xue, B. Gerstbrein, M. Driscoll, and W. R. Schafer. 2003. In Vivo imaging of C. elegans mechanosensory neurons demonstrates a specific role for the MEC-4 channel in the process of gentle touch sensation. *Neuron.* 39:1005–1017.
5. Shimozono, S., T. Fukano, K. D. Kimura, I. Mori, Y. Kirino, and A. Miyawaki. 2004. Slow Ca^{2+} dynamics in pharyngeal muscles in Caenorhabditis elegans during fast pumping. *EMBO Rep.* 5:521–526.
6. Wang, J. W., A. M. Wong, J. Flores, L. B. Vosshall, and R. Axel. 2003. Two-photon calcium imaging reveals an odor-evoked map of activity in the fly brain. *Cell.* 112:271–282.
7. Liu, L., O. Yermolaieva, W. A. Johnson, F. M. Abboud, and M. J. Welsh. 2003. Identification and function of thermosensory neurons in *Drosophila* larvae. *Nat. Neurosci.* 6:267–273.
8. Reiff, D. F., P. R. Thiel, and C. M. Schuster. 2002. Differential regulation of active zone density during long-term strengthening of *Drosophila* neuromuscular junctions. *J. Neurosci.* 22:9399–9409.
9. Reiff, D. F., A. Ihring, G. Guerrero, E. Y. Isacoff, M. Joesch, J. Nakai, and A. Borst. 2005. In vivo performance of genetically encoded indicators of neural activity in flies. *J. Neurosci.* 25:4766–4778.
10. Higashijima, S. I., M. A. Masino, G. Mandel, and J. R. Fetcho. 2003. Imaging neuronal activity during zebrafish behavior with a genetically encoded calcium indicator. *J. Neurophysiol.* 90:3986–3997.
11. Hasan, M. T., R. W. Friedrich, T. Euler, M. E. Larkum, G. Giese, M. Both, J. Duebel, J. Waters, H. Bujard, O. Griesbeck, R. Y. Tsien, T. Nagai, A. Miyawaki, and W. Denk. 2004. Functional fluorescent Ca^{2+} indicator proteins in transgenic mice under TET control. *PLoS Biol.* 2:763–775.
12. Ji, G., M. E. Feldman, K. Y. Deng, K. S. Greene, J. Wilson, J. C. Lee, R. C. Johnston, M. Rishniw, Y. Tallini, J. Zhang, W. G. Wier, M. P. Blaustein, H. B. Xin, J. Nakai, and M. I. Kotlikoff. 2004. Ca^{2+}-sensing transgenic mice: postsynaptic signaling in smooth muscle. *J. Biol. Chem.* 279:21461–21468.
13. Heim, N., and O. Griesbeck. 2004. Genetically encoded indicators of cellular calcium dynamics based on troponin C and green fluorescent protein. *J. Biol. Chem.* 279:14280–14286.
14. Nakai, J., M. Ohkura, and K. Imoto. 2001. A high signal-to-noise Ca^{2+} probe composed of a single green fluorescent protein. *Nat. Biotechnol.* 19:137–141.
15. Filippin, L., P. J. Magalhaes, G. Di Benedetto, M. Colella, and T. Pozzan. 2003. Stable interactions between mitochondria and endoplasmic reticulum allow rapid accumulation of calcium in a subpopulation of mitochondria. *J. Biol. Chem.* 278:39224–39234.
16. Pologruto, T. A., R. Yasuda, and K. Svoboda. 2004. Monitoring neural activity and $[Ca^{2+}]$ with genetically encoded Ca^{2+} indicators. *J. Neurosci.* 24:9572–9579.
17. Gordon, A. M., E. Homsher, and M. Regnier. 2000. Regulation of contraction in striated muscle. *Physiol. Rev.* 80:853–924.
18. Potter, J. D., and J. Gergely. 1975. The calcium and magnesium binding sites on troponin and their role in the regulation of myofibrillar adenosine triphosphatase. *J. Biol. Chem.* 250:4628–4633.
19. Robertson, S. P., J. D. Johnson, and J. D. Potter. 1981. The time-course of Ca^{2+} exchange with calmodulin, troponin, parvalbumin, and myosin in response to transient increases in Ca^{2+}. *Biophys. J.* 34:559–569.
20. Baird, G. S., D. A. Zacharias, and R. Y. Tsien. 1999. Circular permutation and receptor insertion within green fluorescent proteins. *Proc. Natl. Acad. Sci. USA.* 96:11241–11246.
21. Topell, S., J. Hennecke, and R. Glockshuber. 1999. Circularly permuted variants of the green fluorescent protein. *FEBS Lett.* 457:283–289.
22. Nagai, T., S. Yamada, T. Tominaga, M. Ichikawa, and A. Miyawaki. 2004. Expanded dynamic range of fluorescent indicators for Ca^{2+} by circularly permuted yellow fluorescent proteins. *Proc. Natl. Acad. Sci. USA.* 101:10554–10559.
23. Brand, A. H., and N. Perrimon. 1993. Targeted gene expression as a means of altering cell fates and generating dominant phenotypes. *Development.* 118:401–415.
24. Spradling, A. C., and G. M. Rubin. 1982. Transposition of cloned P elements into *Drosophila* germ line chromosomes. *Science.* 218:341–347.
25. Lin, D. M., and C. S. Goodman. 1994. Ectopic and increased expression of fasciclin II alters motoneuron growth cone guidance. *Neuron.* 13:507–523.
26. Rizzo, M. A., G. H. Springer, B. Granada, and D. W. Piston. 2004. An improved cyan fluorescent protein variant useful for FRET. *Nat. Biotechnol.* 22:445–449.
27. Griesbeck, O., G. S. Baird, R. E. Campbell, D. A. Zacharias, and R. Y. Tsien. 2001. Reducing the environmental sensitivity of yellow fluorescent protein. Mechanism and applications. *J. Biol. Chem.* 276: 29188–29194.
28. Pearlstone, J. R., T. Borgford, M. Chandra, K. Oikawa, C. M. Kay, O. Herzberg, J. Moult, A. Herklotz, F. C. Reinach, and L. B. Smillie. 1992. Construction and characterization of a spectral probe mutant of troponin C: application to analyses of mutants with increased Ca^{2+} affinity. *Biochemistry.* 31:6545–6553.
29. Szczesna, D., G. Guzman, T. Miller, J. Zhao, K. Farokhi, H. Ellemberger, and J. D. Potter. 1996. The role of the four Ca^{2+} binding sites of troponin C in the regulation of skeletal muscle contraction. *J. Biol. Chem.* 271:8381–8386.
30. Fortes de Valencia, F., A. A. Paulucci, R. B. Quaggio, A. C. Rasera da Silva, C. S. Farah, and F. Castro Reinach. 2003. Parallel measurement of Ca^{2+} binding and fluorescence emission upon Ca^{2+} titration of recombinant skeletal muscle troponin C. Measurement of sequential calcium binding to the regulatory sites. *J. Biol. Chem.* 278:11007–11014.
31. Tikunova, S. B., D. J. Black, J. D. Johnson, and J. P. Davis. 2001. Modifying Mg^{2+} binding and exchange with the N-terminal of calmodulin. *Biochemistry.* 40:3348–3353.
32. Davis, J. P., J. A. Rall, P. J. Reiser, L. B. Smillie, and S. B. Tikunova. 2002. Engineering competitive magnesium binding into the first EF-hand of skeletal troponin C. *J. Biol. Chem.* 277:49716–49726.
33. Procyshyn, R. M., and R. E. Reid. 1994. A structure/activity study of calcium affinity and selectivity using a synthetic peptide model of the helix-loop-helix calcium-binding motif. *J. Biol. Chem.* 269:1641–1647.
34. Marsden, B. J., G. S. Shaw, and B. D. Sykes. 1990. Calcium binding proteins. Elucidating the contributions to calcium affinity from an analysis of species variants and peptide fragments. *Biochem. Cell Biol.* 68:587–601.
35. Trigo-Gonzalez, G., G. Awang, K. Racher, K. Neden, and T. Borgford. 1993. Helix variants of troponin C with tailored calcium affinities. *Biochemistry.* 32:9826–9831.
36. Miyawaki, A., J. Llopis, R. Heim, J. M. McCaffery, J. A. Adams, M. Ikura, and R. Y. Tsien. 1997. Fluorescent indicators for Ca^{2+} based on green fluorescent proteins and calmodulin. *Nature.* 388:882–887.
37. Nagai, T., A. Sawano, E. S. Park, and A. Miyawaki. 2001. Circularly permuted green fluorescent proteins engineered to sense Ca^{2+}. *Proc. Natl. Acad. Sci. USA.* 98:3197–3202.
38. Ohkura, M., M. Matsuzaki, H. Kasai, K. Imoto, and J. Nakai. 2005. Genetically encoded bright Ca^{2+} probe applicable for dynamic Ca^{2+} imaging of dendritic spines. *Anal. Chem.* 77:5861–5869.
39. Jurado, L. A., P. S. Chockalingam, and H. W. Jarrett. 1999. Apocalmodulin. *Physiol. Rev.* 79:661–682.